



Prediction of ground reaction forces during gait based on kinematics and a neural network model



Seung Eel Oh, Ahnryul Choi, Joung Hwan Mun*

Department of Bio-Mechatronic Engineering, College of Biotechnology and Bioengineering, Sungkyunkwan University, 300 Chunchun, Jangan, Suwon, Gyeonggi 440-746, Republic of Korea

ARTICLE INFO

Article history:
Accepted 26 July 2013

Keywords:
Complete gait cycle
Gait model
Prediction of ground reaction force & moment
Inverse dynamic
Artificial neural network

ABSTRACT

Kinetic information during human gait can be estimated with inverse dynamics, which is based on anthropometric, kinematic, and ground reaction data. While collecting ground reaction data with a force plate is useful, it is costly and requires regulated space. The goal of this study was to propose a new, accurate methodology for predicting ground reaction forces (GRFs) during level walking without the help of a force plate. To predict GRFs without a force plate, the traditional method of Newtonian mechanics was used for the single support phase. In addition, an artificial neural network (ANN) model was applied for the double support phase to solve statically indeterminate structure problems. The input variables of the ANN model, which were selected to have both dependency and independency, were limited to the trajectory, velocity, and acceleration of the whole segment's mass centre to minimise errors. The predicted GRFs were validated with actual GRFs through a ten-fold cross-validation method, and the correlation coefficients (R) for the ground forces were 0.918 in the medial–lateral axis, 0.985 in the anterior–posterior axis, and 0.991 in the vertical axis during gait. The ground moments were 0.987 in the sagittal plane, 0.841 in the frontal plane, and 0.868 in the transverse plane during gait. The high correlation coefficients (R) are due to the improvement of the prediction rate in the double support phase. This study also proved the possibility of calculating joint forces and moments based on the GRFs predicted with the proposed new hybrid method. Data generated with the proposed method may thus be used instead of raw GRF data in gait analysis and in calculating joint dynamic data using inverse dynamics.

© 2013 Elsevier Ltd. All rights reserved.

1. Introduction

Ground reaction forces and moments (GRF&M) are very important in gait analysis to study the kinetic interaction with the ground and to estimate joint kinetics by inverse dynamics (Winter, 1991). GRF&M data are usually acquired using a force platform. But this technique is limited because force platforms only allow collecting a few steps, making it difficult to analyse fluctuations in gait patterns (Chau et al., 2005; Senden et al., 2009). Moreover, force platforms should be properly fixed to the ground and are therefore not available everywhere. For these reasons, various methods have been proposed to predict the GRF&M during gait based on the subject's kinematics (Ren et al., 2005, 2008; Ligris et al., 2011; Xiang et al., 2011).

The human gait is divided into a single support phase (SSP) and a double support phase (DSP). Although the DSP only constitutes 20 to 25% of one gait cycle, it is valuable for the diagnosis of disease and assessment of gait (Davis and Cavanagh, 1993; Goldberg et al., 2006). While GRF&M can be accurately predicted

by Newtonian mechanics in SSP since GRF only acts as an external force, during the DSP, when both legs and the ground surface form a closed loop, the GRF&M under each foot cannot be determined; thus, some assumptions or applications of other methods are needed to address this limitation; hence recently published papers have focused on the prediction of GRF&M during DSP. Ren et al. (2005) proposed a linear transfer relationship model based on empirical data to solve the statically indeterminate problem that occurs during the DSP. Nevertheless, the results were limited to horizontal and vertical forces and the resultant moments. Ren et al. (2008) also proposed the smooth transition assumption (STA) during the DSP. In that study, the GRF&M of whole axes in three-dimensional (3D) space were predicted based on measured 3D kinematic data alone. As a result, reasonably good GRF estimates in the sagittal plane were obtained. However, the relative RMSEs of the estimated GRF&M in the lateral axis and the frontal and transverse planes with relatively small magnitudes were weaker (26% to 33%). The two previous studies by Ren et al. were limited by the assumption that the motions of the right and left limbs during the DSP were symmetrical. Ligris et al. (2011) estimated the GRFs during the DSP using a foot-ground contact model (FCM)-based optimisation method. Their proposed method

* Corresponding author. Tel.: +82 31 299 4820; fax: +82 31 299 4825.
E-mail address: jmun@skku.edu (J.H. Mun).

resulted in better correlation coefficients and RMSEs than the STA method. However, they did not resolve the issue of clinical application because discontinuities in the predicted values occurred during the optimisation process (Lugris et al., 2011). Using an optimisation-based predictive dynamics approach, Xiang et al. (2011) calculated the joint torques and the GRFs during asymmetric gait motion. However, in the optimisation-based method, the objective function only partially represents the human neural control system and has drawbacks in predicting a completely natural motion (Xiang et al., 2011). In a comprehensive manner, the methods used in the prior studies that were related to the GRF prediction still have limitations for clinical application due to the assumptions regarding human movements and drawbacks in application techniques.

According to Liu et al. (1999), the predicted results were considered excellent if the cross-correlation coefficient is greater than 0.9 and the relative RMSE is smaller than 15%. Nonetheless, there have been few studies on joint force and moment predictions without the use of force plates during gait. However, while the SSP prediction using a conventional method already shows high accuracy, the gait cycle has a statically indeterminate structure during the DSP, and new algorithms are needed for more accurate reaction force estimations.

ANNs are an extraordinarily flexible tool for nonlinear modelling and are especially useful in gait analysis (Kaczmarczyk et al., 2009). Many studies (Holzreiter and Köhle, 1993; Barton and Lees, 1995, 1997; Lafuente et al., 1998; Schöllhorn, 2004) have shown that ANNs can be useful in predicting or distinguishing gait patterns. Recently, new studies predicting lower body joint loads using an ANN instead of an inverse dynamic approach but have been reported (Favre et al., 2012; Liu et al., 2009). However, typically an ANN needs training data to make a prediction, and it has a difficulty in making decisions without the training data (Vijayakumar and Ramamurthy, 2013).

The purpose of this study is to develop an improved method for predicting GRF&M for a normal gait with high accuracy, and without the need for GRF-measuring devices during level walking (especially during the DSP in a gait). To verify the proposed method, normal gait experiments were carried out on force plates (to collect data of the normal gait with the ease of data acquisition), and the instrument-measured and predicted results were compared. In addition, the same experimental gait dataset obtained in our study was applied to the STA method (Ren et al., 2008), and then we determined whether the method suggested in this study was better than previously developed approaches. The goal of this study is to provide basic research with a verified novel method.

2. Materials and Methods

2.1. Subjects

Forty-eight subjects (28 males and 20 females, age: 25.4 ± 3.1 years; height: 1.72 ± 0.07 m; weight: 66.2 ± 7.5 kg) with no history of musculoskeletal disorders volunteered for the study in the BME laboratory at Sungkyunkwan University.

The local ethics committee approved the study protocol, and informed consent was obtained from all subjects before the study. Of the 48 participants, 43 were randomly selected and used to collect training data for the ANNs, and the remaining subjects were used to collect validation data.

2.2. Instrumentation

The 3D kinematics of 35 reflective markers placed on each subject's body (modified Helen Hayes marker set) were recorded at 120 Hz using six MCAM2 cameras, a Vicon 460 motion analysis system (Vicon Motion Systems, Oxford, UK), and SB-Clinic software (SWING BANK Ltd., Korea). The global X-axis was set to the right, the Y-axis was in the direction of progression, and the Z-axis was vertical. Ground reaction data were recorded synchronously with kinematics at 1080 Hz from two force plates (AMTI, Model OR6-6-2000, MA, USA) that were fixed at the centre of a 10-m-long walkway, but were not apparent to the subjects.

2.3. Experimental protocol and data processing

Subjects were asked to walk barefoot at their own preferred walking speed. The subjects were given sufficient training trials before the recording session. The motion was repeated at least five times and only one arbitrary experimental data set per subject was used for training and validating the neural network. Fifteen rigid segments (head, thorax, humeri, radii, hands, pelvis, femora, tibiae, and feet) were modelled using commercial software, BodyBuilder v3.6, the PlugInGait model (Vicon Motion System, Oxford, UK), and the 3D position data of the markers were recorded. Motion information on the centre of mass of each segment was acquired. Both the kinematic and GRF datasets were low-pass filtered with a 4th-order Butterworth filter using a cut-off frequency of 6 Hz to remove noise. The cut-off frequency was determined based on a previous study (Winter, 2009). Also, the gait event timings were determined using the foot velocity algorithm method, which is based on kinematic data without force plates (O'Connor et al., 2007). The schematic of the overall GRF prediction procedure is shown in Fig. 1.

2.4. Single support phase: conventional method

Since the only external forces acting in a human body during a SSP are GRFs, a traditional method that calculates the GRFs inversely by subtracting the gravitational acceleration from segmental acceleration for each body segment was applied (Siegler and Liu, 1997). Since the Newtonian mechanics-based method already reports high prediction accuracy, the method used in this study is the same as the method used to predict a SSP in a preceding study (Ren et al., 2008). In this regard, all components of the calculated GRFs were computed at the ground surface in the vertical direction from the mass centre of the ankle segment.

2.5. Double support phase: artificial neural network method

Because both legs and the ground surface form a closed loop during the DSP, the redundant system was not able to resolve to a solution by the application of the conventional method detailed in Section 2.4 to determine indeterminate problems. Therefore, after performing Section 2.3, which was done to determine the GRFs without the use of force plates during the DSP, an ANN model was constructed.

In this study, a feed-forward network with one input layer, one hidden layer and one output layer was used to predict the GRF&M for F_x , F_y , F_z , M_x , M_y , and M_z . The network utilised a back-propagation algorithm and the gradient steepest descent method (Schalkoff, 1997). The hidden layer with three nodes consisted of a bipolar sigmoid transfer function. The gait data of 43 randomly-selected subjects (one trial per training subject) among the total of 48 subjects are considered in the ANN training, and the remaining 5 subjects (one trial per validation subject) were used as a test sample to validate the developed ANN.

The predictive ability of the ANN model is strongly affected by the suitable selection of input variables (Fernando et al., 2009; Noori et al., 2011). Among the

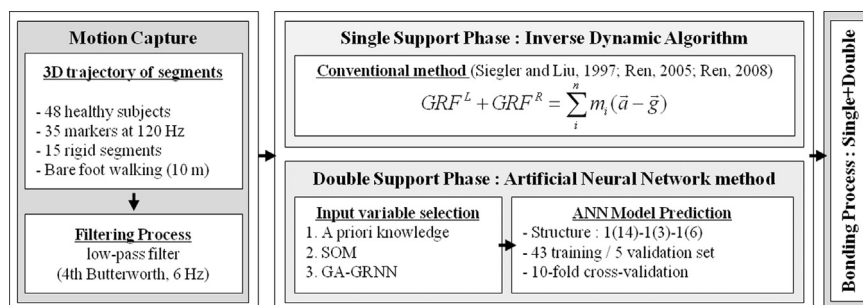


Fig. 1. Flowchart of the process for predicting ground reaction forces and moments.

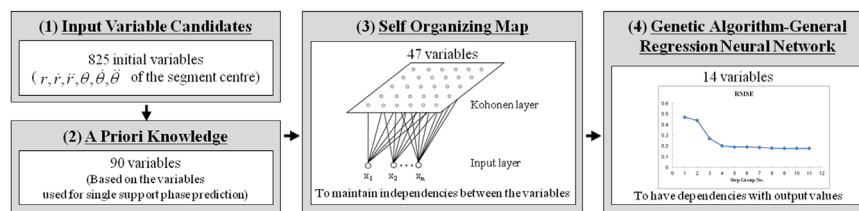


Fig. 2. Schematic of the variable extraction process.

Table 1
The 14 inputs of the neural network.

Type	Unit	Variable
Trajectory	m	Left elbow joint centre in X-axis Left shoulder joint centre in Y-axis Right wrist joint centre in Z-axis Left foot segment mass centre in X-axis Pelvis segment mass centre in X-axis Left femur segment mass centre in Y-axis Right tibia segment mass centre in Z-axis
Acceleration	m/s ²	C7/T1 joint centre in Y-axis Right elbow joint centre in Z-axis Right tibia segment mass centre in X-axis Right foot segment mass centre in Y-axis Right femur segment mass centre in Y-axis Left foot segment mass centre in Z-axis Pelvis segment mass centre in Z-axis

key error sources affecting the accuracy of the human model analysis while walking, parameters such as segment angles, body segment parameters, and segment inertial forces accumulate more error than the locations of the joint centres of rotation, force measurements, motion marker noise and segmental accelerations (Rao et al., 2006; Riemer et al., 2008). Therefore, the initial candidates from the entire range of input variables for the ANN were limited to the raw data for the walking motion, trajectory, velocity and acceleration of the segment centres.

The input variable selection process consisted of 4 steps as shown in Fig. 2, and the details for each process are as follows:

- (1) Since the GRF varies with the movement of the human body, all of the motion-related data can be used as input variables of the ANN for predicting the GRF. The initial candidates of the entire set of input variables can be summarised into approximately 825.
- (2) The initial input candidates have a high dimensionality, which may lead to a long calculation time when all are used. It was possible to select primary input variables that strongly affect on the ground reaction force data based on the variables used in the Newtonian mechanics formula for SSP prediction. Consequently, the dimensionality of the variables was reduced to 90 using a priori knowledge.
- (3) Among the variables selected in the preceding process using a priori knowledge, there can be variables that are highly correlated with each other. The self-organizing map technique was applied to acquire dependency between the 90 dimensions of variables (Kohonen, 1982; Islam and Kothari, 2000); then, the variables with high correlation were removed, reducing the dimension by sampling 47 representative variables among the variables with high similarity.
- (4) Since the relationship between the 47 selected independent variables and the ANN output is still unknown, a genetic algorithm-general regression neural network was applied, and 14 variables with high correlations to the output were selected (Bowden et al., 2005). The final 14 selected variables of Table 1 have acquired independency, and also have dependency that minimises error to the output.

We prepared time series data for the 14 selected input variables. The input variables were subjected to only a filtering process so that they maintained their raw characteristics. The structure of the ANN is shown in Table 2 in detail.

2.6. Bonding of the single and double support phases

The bonding process accompanying a spline operation was necessary to combine the single and double support phases because different methods were applied in the single (conventional method) and double (ANN method) support phases. Since the two phases are mutually disjointed, and there can be inevitable discontinuity by the ANN characteristic that predicts the whole time period individually, the spline process was needed throughout the entire interval to solve

the discontinuity of the combined points (Gaggero et al., 2013). After connecting in parallel, cubic spline interpolation was used.

2.7. Data analysis

Experimental data from 43 subjects were modelled as the training set for the ANN, and data from the remaining five subjects were used to validate the results. To validate the performance of the model and estimate the robustness, the 10-fold cross-validation process was used, but was limited to the DSP (Karimi et al., 2006; Delen et al., 2005). The data sets for the training and verification were randomly selected, and thus should not be dependent; in addition, we tried to improve the model objectivity by processing each of the 10 repetitions of the cross-validation runs separately. To quantify the differences between the predicted and measured values, the correlation coefficients (R) and RMSEs were determined.

$$RMSE = \sqrt{\frac{1}{T} \int_0^T [u_1(t) - u_2(t)]^2 dt} \quad (1)$$

where $u_1(t)$ and $u_2(t)$ are the predicted and measured values, respectively, and T is each subject's total time of movement.

The relative RMSE with respect to the average peak-to-peak amplitude between two values was calculated as follows:

$$relative\ RMSE = \frac{RMSE}{1/2[\sum_{i=1}^n (\max(u_i(t)) - (\min u_i(t))]} \times 100\% \quad (2)$$

The range for the maximum and minimum was restricted to the range in which yielding values exist. It was set during the stance phase for GRF&M calculation, and was set during the entire gait cycle for joint loads calculation.

3. Results

3.1. Ground reaction forces and moments

The measured kinematics during level walking were similar to general patterns observed in previous studies (Buczek et al., 2010; Mills et al., 2007; Nester et al., 2003; Kadaba et al., 1990). To present the accuracy of the GRF&M prediction model objectively, the prediction results were divided between the SSP and DSP, where different methods were applied, and the entire single gait cycle.

3.1.1. Single support phase

To predict the GRFs of the SSP alone with the kinematic data from the ground level gait, the conventional method from a prior study (Ren et al., 2008) was used. Fig. 3 shows the GRF&M predicted during the SSP. Table 3 shows the results obtained when reproduced by the method of the preceding study. As shown in Fig. 3, the predicted GRF&M in the SSP appear to closely conform to the values measured by the force platform. According to Table 3, the correlation coefficients between the predicted and measured GRFs were 0.736, 0.978, and 0.988 for the medial/lateral, anterior/posterior, and vertical axes, respectively. The predicted GRMs were 0.996, 0.815, and 0.854 in the sagittal, frontal, and transverse planes, respectively. The results of the predicted GRF&M were similar to the results of previous studies (Ren et al., 2008).

3.1.2. Double support phase

The human body becomes a statically indeterminate structure during a DSP in gait; thus, an ANN model was used to solve this problem. During a one-gait cycle, the DSP occurs twice, before and

Table 2
Artificial neural network structure.

Items	Details
Subjects	Healthy subjects: 48 people (28 males, 20 females)
Training data	Randomly selected 43 subjects among the total of 48 subjects One gait cycle of data, 100% normalised, of the randomly selected 43 subjects \times 14 input variables (14×4300), and 6 corresponding GRF outputs: F_x, F_y, F_z, M_x, M_y , and M_z (6×4300)
Validation data	The dataset of the remaining 5 people who were not selected as part of the training group
Validation method	10-fold cross-validation
Input	One gait cycle of data, 100% normalised, of the 5 people who were not used in model learning \times 14 input variables (14×500)
Output	Six GRF data outputs: F_x, F_y, F_z, M_x, M_y , and M_z (6×500)
ANN structure (1-1-1)	1 input layer: 14 nodes (14 variables among the total, secured independency/dependency) 1 hidden layer: 3 nodes (decide by substituting at $1 \sim 2n+1$ one by one, following the Kolmogorov theorem) 1 output layer: 6 nodes (GRF outputs: F_x, F_y, F_z, M_x, M_y , and M_z)
ANN conditions	Maximum learning number: 3000/self-weighting: 0.001/learning rate: 0.01/momentum: 0.8/transfer function: bipolar sigmoid function
Input pre-processing	Filtering (low-pass filtered with a fourth-order Butterworth filter using a cut-off frequency of 6 Hz) for feature preservation, based on the coordinates and angular values of the initial posture; normalise one gait cycle to 100%; scale input from -1 to 1

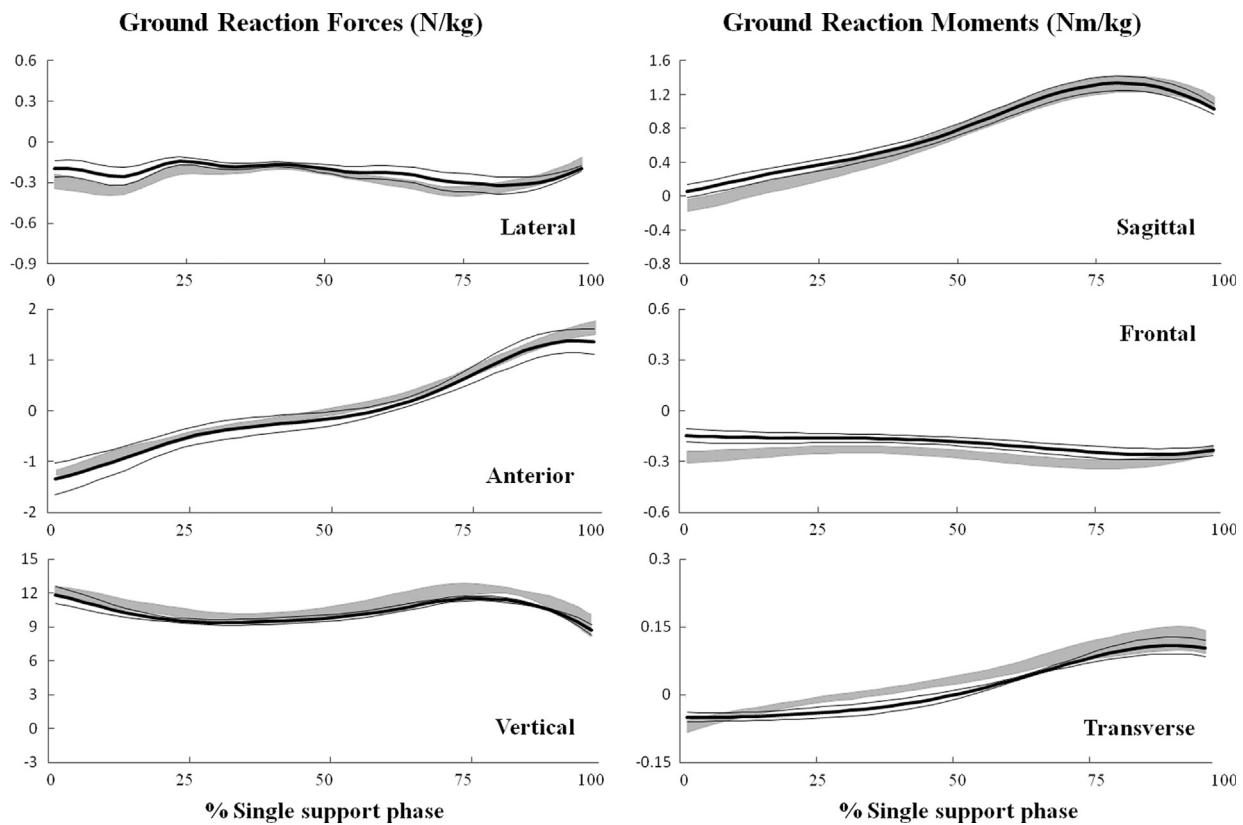


Fig. 3. Predicted GRF&M from the conventional method (mean (thick line) \pm 1 SD (thin lines)) vs. measured GRF&M (mean \pm 1 SD (shaded area)) in the single support phase.

Table 3
Correlation coefficients (R) and absolute and relative RMSEs (Mean (SD)) for ground reaction forces (N/kg) and moments (Nm/kg) during the single support phase.

Method	Reimplemented method (inverse dynamic algorithm adopted from Ren et al., 2008)						
	Participants $N=48$						
Axes	R	RMSE (N/kg)	rRMSE (%)	Planes	R	RMSE (Nm/kg)	rRMSE (%)
Lateral	0.736	0.051 (0.034)	26.2 (4.0)	Sagittal	0.996	0.078 (0.043)	6.0 (2.3)
Anterior	0.978	0.071 (0.028)	2.6 (0.7)	Frontal	0.815	0.052 (0.013)	53.7 (9.7)
Vertical	0.988	0.352 (0.114)	11.3 (2.1)	Transverse	0.854	0.022 (0.012)	12.9 (4.6)

after the SSP, within the stance phase. Fig. 4 shows the GRF&M predicted during the first and second double support phases, and Table 4 compares the results of applying a previously published

algorithm (Ren et al., 2008) and our new algorithm using the same gait data. As shown in Fig. 4, the GRF&M during the DSP predicted by the ANN model seem to match in the magnitude and overall patterns

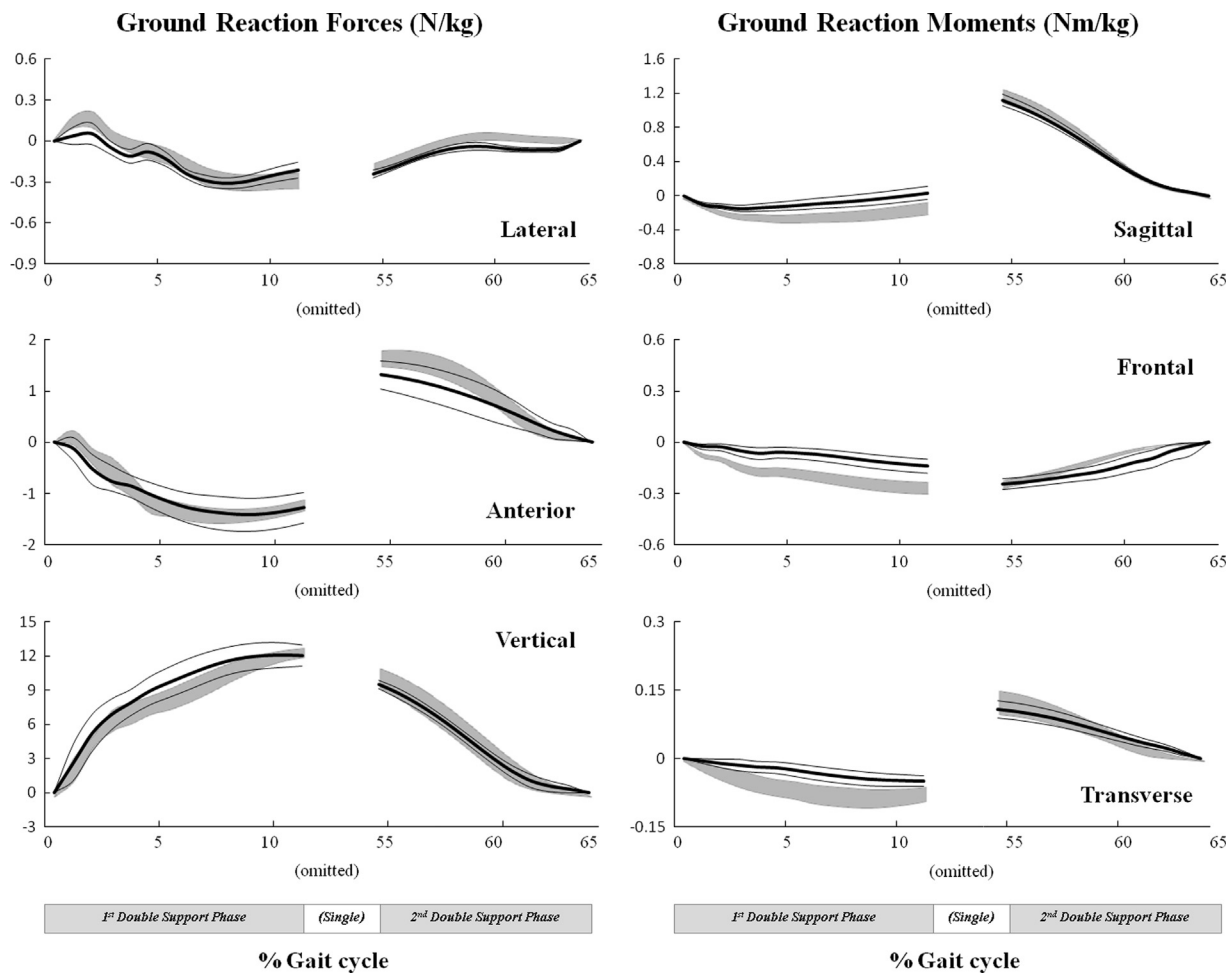


Fig. 4. Predicted GRF&M from the ANN method (mean (thick line) \pm 1 SD (thin lines), described as the mean of 10 folds) vs. measured GRF&M (mean \pm 1 SD (shaded area)) in the double support phase.

Table 4
Correlation coefficients (*R*) and absolute and relative RMSEs for ground reaction forces (N/kg) and moments (Nm/kg) and maximum/minimum values for each category (shaded areas) during double support phase.

Method	Smooth transition assumption (method adopted from Ren et al., 2008)			New hybrid method (proposed in this study)		
Participants	<i>N=5 (10-fold cross-validation results, the same experimental walking data acquired in this study)</i>					
Axes/ Planes	<i>R</i>	RMSE (N/kg or Nm/kg)	rRMSE (%)	<i>R</i>	RMSE (N/kg or Nm/kg)	rRMSE (%)
Lateral	0.648	0.168(0.030)	21.4(2.3)	0.965	0.046(0.024)	11.7(2.0)
Anterior	0.847	0.437(0.056)	11.3(1.0)	0.986	0.125(0.043)	4.4(0.7)
Vertical	0.909	0.787(0.153)	6.9(0.8)	0.990	0.566(0.148)	4.7(0.8)
Sagittal	0.956	0.166(0.071)	11.2(1.9)	0.986	0.056(0.037)	4.3(1.0)
Frontal	0.232	0.153(0.032)	35.5(4.6)	0.809	0.073(0.035)	29.4(4.7)
Transverse	0.714	0.030(0.010)	22.0(2.8)	0.884	0.017(0.008)	9.6(2.7)

as compared with the measured values. According to Table 4, the correlation coefficients between the predicted and measured GRFs in the medial/lateral, anterior/posterior, and vertical axes were 0.965, 0.986, and 0.990, respectively. The correlation coefficients of the predicted GRMs in the sagittal, frontal, and transverse planes were 0.986, 0.809, and 0.884, respectively, which are significant

improvements achieved by applying the ANN method proposed in this study, as compared to the method of the preceding study(Ren et al., 2008).

3.1.3. Whole gait cycle

By colligating the SSP, where the conventional method was used, and the DSP, where the ANN method was used, the stance phase was composed. Fig. 5 shows the predicted GRF&M determined using the new hybrid method (NHM) developed in this study for one gait cycle, and it also shows a comparison between the predicted results and the values measured by the force plates during the same interval. As shown in Fig. 5, the predicted GRF&M had no discontinuities between the phases.

Table 5 compares the GRF and GRM results of the three methods. The first six columns show the original values, which were cited from two different studies (Ren et al., 2008; Lgrís et al., 2011); the last six columns show a comparison of results calculated with the STA (Ren et al., 2008) and our newly developed NHM based on the same experimental gait data set. The foot-ground contact model (Lgrís et al., 2011) was not re-implemented due to lack of information.

According to Table 5, in predicting the GRFs using the developed NHM, the correlation coefficients (*R*) between the predicted and measured values showed very high correlation compared to previously published results, as shown in the third column from the right: 0.918 in the medial–lateral axis, 0.985 in the anterior–posterior

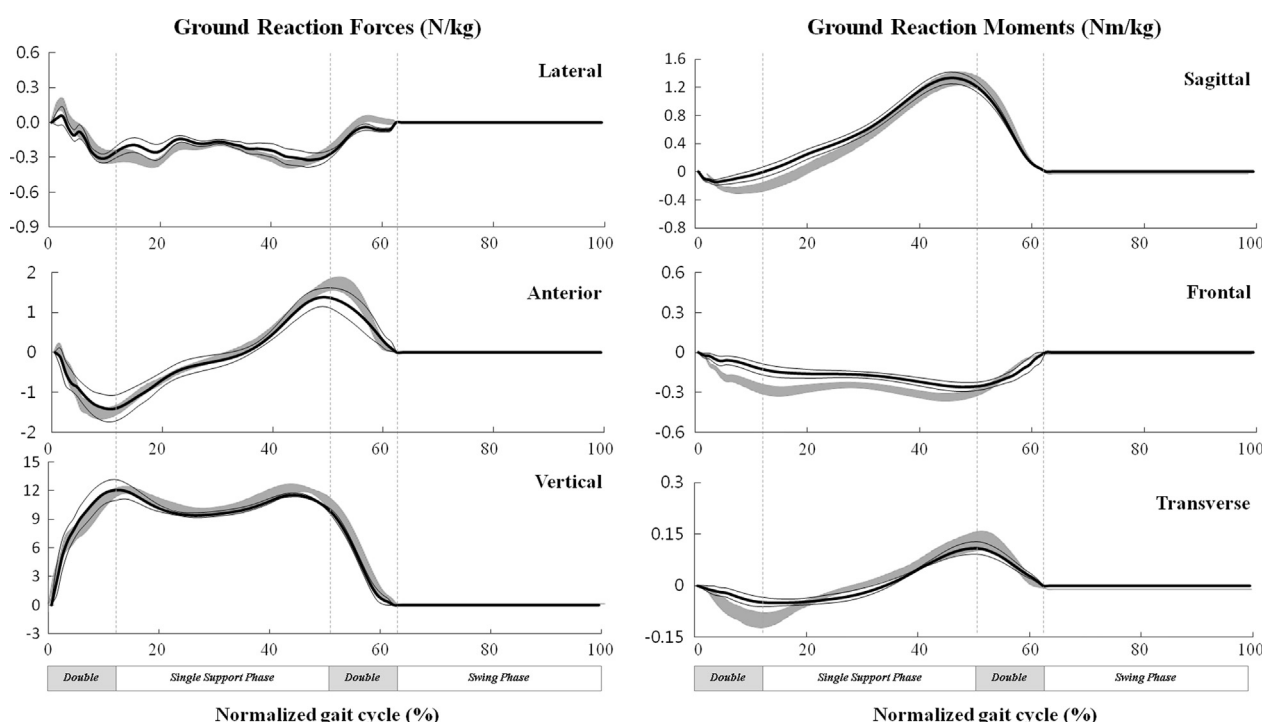


Fig. 5. Predicted ground forces and moments normalised by body mass (mean (thick line) \pm 1 SD (thin lines), described as the mean of 10 folds) compared with force plate data (mean \pm 1 SD (shaded area)).

Table 5

Correlation coefficient (R) and absolute and relative RMSEs (mean (SD)) for ground reaction forces (N/kg) and maximum/minimum values for each category (shaded area) during one entire gait cycle.

Method	Smooth transition assumption (Results from Ren et al., 2008)			Foot-ground contact model ^a (Results from Lugić et al., 2011)			Smooth transition assumption (Method adopted from Ren et al., 2008)			New hybrid method (Method proposed in this study)		
Participants	N=3			N=1			N=5 (10-fold cross-validation results)					
Axes/Planes	R	RMSE (N/kg or Nm/kg)	rRMSE (%)	R	RMSE (N/kg or Nm/kg)	rRMSE (%)	R	RMSE (N/kg or Nm/kg)	rRMSE (%)	R	RMSE (N/kg or Nm/kg)	rRMSE (%)
Lateral	-0.191 (0.034)	20.0 (2.7)	-	-	-	-	0.704	0.221 (0.043)	19.8 (2.2)	0.918	0.040 (0.022)	10.9 (1.8)
Anterior	-0.473 (0.068)	10.9 (0.83)	-	-	-	-	0.878	0.437 (0.085)	10.5 (0.8)	0.985	0.154 (0.057)	7.3 (0.8)
Vertical	-0.710 (0.190)	5.6 (1.5)	-	0.687 (-)	-	-	0.913	0.805 (0.202)	6.5 (1.3)	0.991	0.649 (0.182)	5.8 (1.0)
Sagittal	-0.199 (0.106)	12.2 (4.8)	-	0.241 (-)	-	-	0.978	0.193 (0.098)	11.7 (3.4)	0.987	0.081 (0.045)	9.9 (1.9)
Frontal	-0.148 (0.013)	32.5 (4.3)	-	0.154 (-)	-	-	0.677	0.105 (0.026)	33.3 (4.5)	0.841	0.052 (0.029)	22.8 (4.9)
Transverse	-0.039 (0.015)	26.2 (9.4)	-	-	-	-	0.829	0.039 (0.018)	31.0 (6.8)	0.868	0.032 (0.018)	25.5 (4.5)

axis, and 0.991 in the vertical axis. In addition, based on the results of the RMSE analysis between the predicted and measured values during the single gait cycle, results of 0.040–0.649 N/kg were obtained using the NHM. Also, the GRMs based on the NHM were highly correlated in every plane, with an R of 0.987 in the sagittal, 0.841 in the frontal, and 0.868 in the transverse planes. The RMSEs for the GRMs ranged from 0.032 to 0.081 Nm/kg, and these results are markedly improved over a previous study (Table 5). The relative RMSEs for the GRMs (9.9 to 25.5%) were also similar or better for all axes as compared to the previous study.

3.2. Resultant joint forces and net muscle moments

The resultant joint forces and moments can be estimated using a multi-segment model and inverse dynamics, which is based on the GRFs calculated using the NHM. When the previously predicted GRFs were considered as the only external forces, the joint forces and moments that were translated to each joint (ankle, knee, and hip) of the lower limbs could be obtained using Vicon's

BodyBuilder v3.6 and PlugInGait models (Vicon Motion Systems, Oxford, UK). The joint forces and moments obtained using the original and predicted GRFs are shown in Figs. 6 and 7.

Table 6 shows the absolute and relative RMSEs and the correlation coefficients of each of the acquired joint forces and moments based on the measured and predicted GRFs. The first three columns of Table 6 show the original values that were cited from another study (Ren et al., 2008) and the last six columns show the results comparing the STA and our newly developed NHM based on the same experimental gait data set during one gait cycle. Also, the joint force RMSE calculated using two GRFs (with and without force plate data) during one gait cycle showed more than 0.1 N/kg of improvement along every axis when the results of the NHM were compared to the STA results. The relative RMSEs varied depending on the axis, but on average, an improvement of roughly 7% was observed. The absolute and relative RMSEs of the joint moments also improved when NHM was applied rather than the STA method, except in the ankle's sagittal plane, where the results were similar.

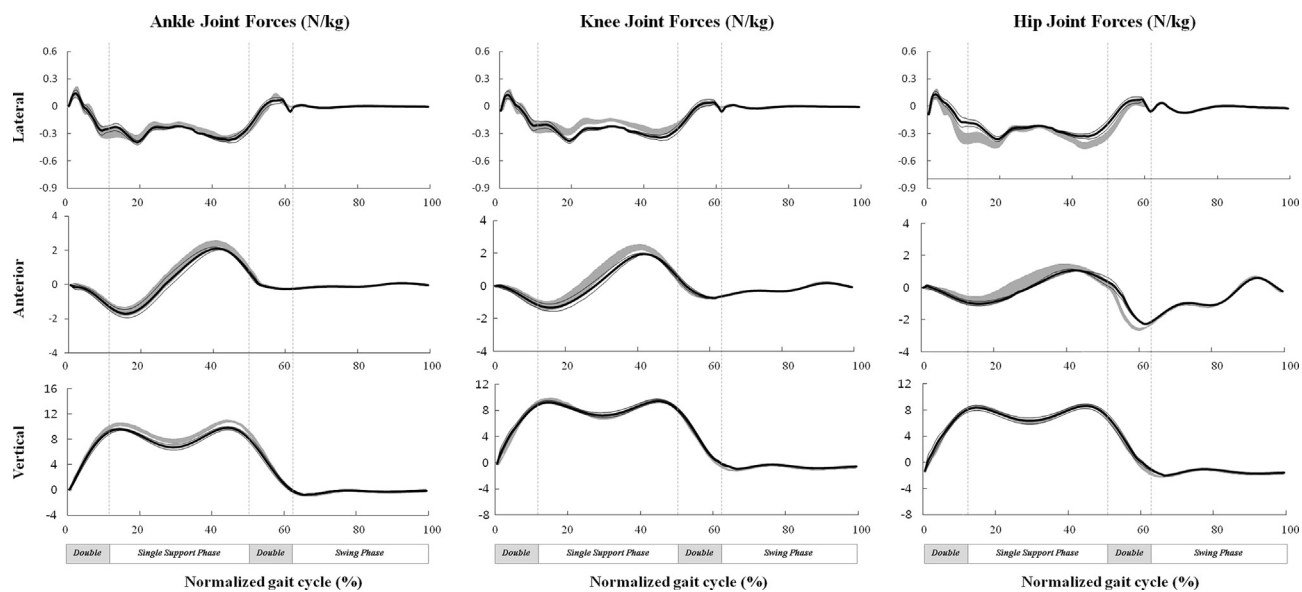


Fig. 6. Estimated resultant joint forces using predicted GRFs (mean (thick line) \pm 1 SD (thin lines), normalised by body mass and described as the mean of 10 folds) compared with joint forces calculated based on the original GRF data (mean \pm 1 SD (shaded area)).

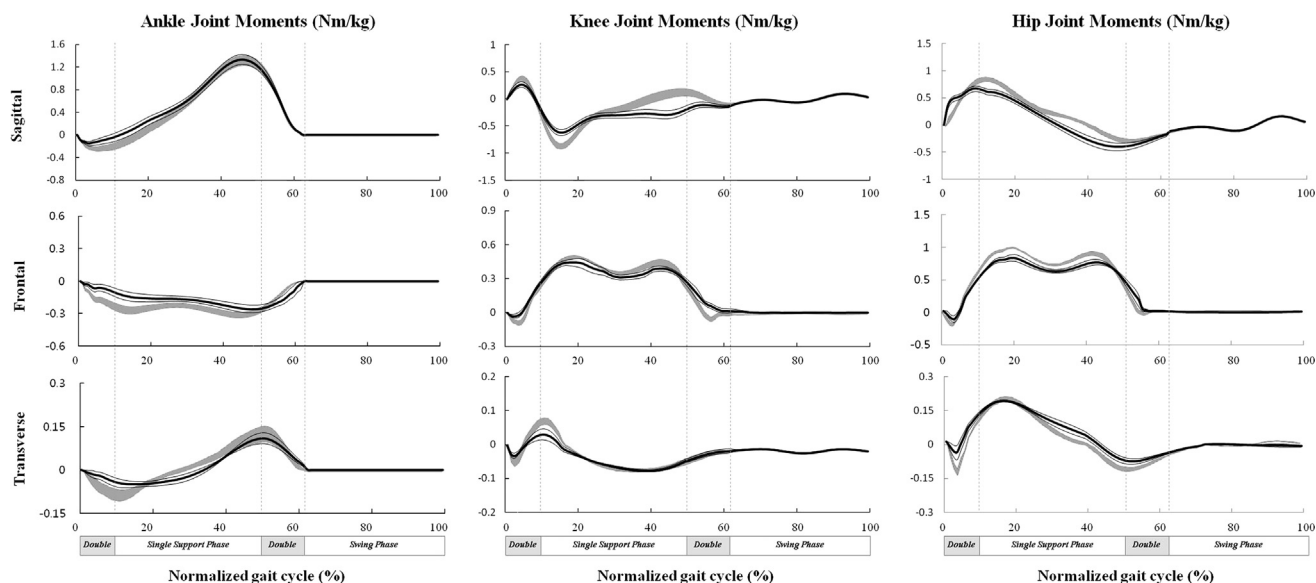


Fig. 7. Estimated joint net muscle moments using predicted GRFs (Mean (thick line) \pm 1 SD (thin lines), normalised by body mass and described as the mean of 10 folds) compared with moments calculated based on original GRF data (mean \pm 1 SD (shaded area)).

4. Discussion

When clinically analysing the gait, GRF values are very important as inputs for the joint mechanics (Kadaba et al., 1989). However, the ground reaction can only be measured by devices such as force platforms, and the spatial constraints of these devices cause several limitations in the gait analysis of special cases (O'Connor et al., 2007). A method for predicting the reaction force without a force platform could avoid these limitations, which would be a significant advantage. For these reasons, there have been several studies predicting the GRF&M from the motion data of subjects alone (Ren et al., 2005; Ren et al., 2008; Lugić et al., 2011; Xiang et al., 2011) as well as predicting the joint load in motion using ANN (Favre et al., 2012; Liu et al., 2009).

The ANN applied to predict GRFs in the DSP was designed as a multi-layer with '14-3-6' nodes. The 14 input variables were selected among 825 initial candidates of the entire range of input variables, which were based on gait kinematic data and a priori knowledge; the

self-organizing map technique and genetic algorithm-general regression neural network processes were used to select the final set of input variables. In addition, according to the theorem of Kolmogorov, the numbers of hidden layers and neurons were decided with an empirical method base (Kolmogorov, 1957).

In the predicted GRF&M, there was no data discontinuity between the phases. As shown in Fig. 5, there were no discontinuities found at the junctions where the two different methods were applied for one gait cycle. This is an improvement to the foot-ground contact method with discontinuity (Lugić et al., 2011), and the symptom is believed to occur due to the filtering process used on the whole section of the predicted value.

According to Tables 3–6, the results reported in prior publications (Ren et al., 2008) and results obtained in this study with re-implemented previously-used methods were compared in RMSE and rRMSE, and were quite similar. Some of the inconsistencies are thought to have occurred due to the different measured information of the subjects and filtering options.

Table 6

Correlation coefficients (R) and absolute and relative RMSEs (mean (SD)) for joint forces (N/kg), joint moments (Nm/kg), and maximum/minimum values for each category (shaded area).

Method	Smooth transition assumption			Smooth transition assumption			New hybrid method		
	(Results from Ren et al., 2008)			(Method adopted from Ren et al., 2008)			(Method proposed in this study)		
Participants	N=3			N=5 (10-fold cross-validation results)					
Quantities	R	RMSE (N/kg or Nm/kg)	rRMSE (%)	R	RMSE (N/kg or Nm/kg)	rRMSE (%)	R	RMSE (N/kg or Nm/kg)	rRMSE (%)
<i>Joint forces</i>									
<i>Hip</i>									
Lateral	–	0.203 (0.038)	23.3 (3.5)	0.772	0.303 (0.021)	27.7 (2.9)	0.852	0.128 (0.021)	12.6 (2.0)
Anterior	–	0.480 (0.073)	21.8 (0.5)	0.787	0.503 (0.084)	21.0 (2.2)	0.938	0.434 (0.068)	6.4 (1.1)
Vertical	–	0.713 (0.193)	5.4 (1.5)	0.839	0.940 (0.219)	6.1 (1.5)	0.979	0.578 (0.165)	2.8 (1.3)
<i>Knee</i>									
Lateral	–	0.186 (0.031)	20.4 (2.5)	0.804	0.294 (0.016)	24.2 (2.8)	0.892	0.092 (0.023)	10.2 (1.3)
Anterior	–	0.470 (0.063)	14.0 (1.1)	0.813	0.564 (0.078)	12.6 (1.6)	0.965	0.348 (0.060)	5.3 (1.9)
Vertical	–	0.703 (0.187)	5.6 (1.5)	0.843	0.933 (0.212)	6.3 (1.6)	0.985	0.590 (0.167)	2.9 (1.3)
<i>Ankle</i>									
Lateral	–	0.183 (0.030)	20.1 (2.7)	0.815	0.291 (0.015)	23.3 (2.0)	0.909	0.054 (0.023)	10.3 (1.7)
Anterior	–	0.468 (0.060)	11.4 (0.9)	0.835	0.494 (0.075)	9.9 (1.3)	0.983	0.222 (0.055)	7.9 (0.8)
Vertical	–	0.701 (0.186)	5.5 (1.5)	0.851	0.931 (0.212)	6.3 (1.6)	0.988	0.644 (0.185)	4.9 (1.4)
<i>Joint moments</i>									
<i>Hip</i>									
Sagittal	–	0.469 (0.067)	20.9 (2.1)	0.868	0.582 (0.038)	19.7 (1.7)	0.931	0.056 (0.041)	9.7 (2.0)
Frontal	–	0.106 (0.008)	9.9 (0.9)	0.756	0.128 (0.016)	9.5 (1.4)	0.888	0.052 (0.006)	5.1 (0.9)
Transverse	–	0.051 (0.006)	15.0 (1.2)	0.751	0.062 (0.006)	15.2 (1.1)	0.788	0.029 (0.040)	12.0 (1.0)
<i>Knee</i>									
Sagittal	–	0.307 (0.056)	18.7 (2.9)	0.919	0.360 (0.043)	15.7 (1.9)	0.936	0.020 (0.007)	8.1 (1.8)
Frontal	–	0.100 (0.017)	15.3 (2.8)	0.724	0.125 (0.012)	14.0 (2.1)	0.880	0.033 (0.019)	6.4 (1.6)
Transverse	–	0.042 (0.012)	25.4 (5.1)	0.683	0.059 (0.011)	29.5 (3.9)	0.717	0.043 (0.036)	13.8 (2.7)
<i>Ankle</i>									
Sagittal	–	0.190 (0.112)	9.7 (4.8)	0.941	0.220 (0.057)	10.6 (2.3)	0.980	0.091 (0.052)	10.5 (4.8)
Frontal	–	0.134 (0.012)	35.8 (4.6)	0.672	0.185 (0.017)	38.6 (2.3)	0.840	0.053 (0.028)	22.7 (5.0)
Transverse	–	0.039 (0.015)	26.1 (9.3)	0.796	0.066 (0.011)	37.9 (3.7)	0.853	0.033 (0.022)	25.0 (4.4)

According to Table 5, where the same validation data and filtering options are applied, the results were better for all axes when compared to the results obtained by applying the STA (Ren et al., 2008) and the foot-ground contact model (Lugrís et al., 2011). In the lateral and horizontal axes, which have small magnitudes compared to that of the vertical axis during gait, RMSEs of 0.040 N/kg and 0.154 N/kg, respectively, were found in this study. These improved values are due to differences in the estimation methods applied in the force-transferring mechanism from the trailing foot to the leading foot during the DSP. In the STA method, the transition functions are determined in a semi-empirical fashion based on simple functions, and have limitations in making accurate ground reaction estimations. On the other hand, the learning-based ANN method applied in this study is a particularly sensitive solution for nonlinear problems (Kaczmarczyk et al., 2009) and was effective at estimating even small ground reactions. The relative RMSE values also showed similar levels of improvement.

Furthermore, the GRM prediction results using the NHM were highly correlated in every plane, as shown in Table 5. Nonetheless, the lower moment prediction value compared to that of the force is believed to occur because the moment arising point was assumed to be below the mass centre of the foot segment. The exact centre of pressure cannot be known without a force platform, and the assumption of a centre of pressure location is inevitable for the moment calculation. Consequently, this assumption can lead to an accumulation of errors in the moment prediction values.

The R values of the resultant joint forces and moments from the predicted GRF&M have a tendency to decrease towards the centre of the body. This is believed to be due to cumulative errors in the conventional method, where the calculation of forces and moments proceeds from the proximal to distal joints (Table 6). In particular, better joint force and moment results were found in

the axes with smaller magnitudes; thus, it appears that the NHM has an outstanding effect on predicting subtle changes.

5. Conclusion

Even though the DSP only constitutes 20–25% of one gait cycle, it is valuable for the diagnosis of disease and assessment of gait (Davis and Cavanagh, 1993; Goldberg et al., 2006). Therefore, calculating dynamic information for each joint during the DSP has significant meaning. Nevertheless, the human body becomes a statically indeterminate structure during the DSP, and the problem cannot be solved with general dynamics equations; focused on this particular phase, diverse methods have been applied. Therefore, the authors of this study proposed a NHM that incorporates data learning based on ANN techniques while still taking advantage of the existing method that have a high SSP prediction rate. Through pilot studies, the gait motion input variables that were expected to have the best prediction rate were selected. After applying the ANN model to the DSP, a filtering process was applied to the whole phase to solve the discontinuity in a junction in the SSP. As a result, the predictive performance for the DSP improved greatly; the GRFs predicted without a force plate had correlation coefficients and relative RMSEs of 0.918 and 10.9% in the medio-lateral axis; 0.985 and 7.3% in the vertical axis; and 0.991 and 5.8% in the vertical axis, respectively. In addition, the correlation coefficients of the predicted ground moments were 0.987 in the sagittal plane, 0.841 in the frontal plane, and 0.868 in the transverse plane. The accuracy in predicting ground moments was thus lower than that of the ground forces, which the authors believe was caused by an assumption made for the centre of pressure location. Therefore, for a complete substitution for the force plate, future studies

should combine the methods from this study with the methods from the study on the prediction of centres of pressure during gait. Still, this study provided significantly improved estimated results along axes and planes with small magnitudes (Sofuwa et al., 2005). In addition, the present study proved the applicability of NHM for predicting GRFs for joint force and moment calculations acting on the lower body joints (ankle, knee and hip). The results of this study are expected to be utilised as a substitute for raw GRF data in motion analysis, and as input information for inverse dynamics, which calculates the dynamic information of segments. However, since the GRF was predicted using the ANN, the results in this study still have the general limitations of an ANN; the NHM was applied to gait motions that already had a regular pattern and the ground reaction force estimation was performed for normal gaits. Therefore, additional studies are needed to examine the GRF prediction of random asymmetric motion including different types of disease data by the data-based learning ANN model. Also, further research regarding continuous points is needed so that a smooth curve across the whole phase could be acquired when implementing ANN. In addition, the potential of using this approach to analyse unusual gait motions should be explored through neural network learning of abnormal gait data from patients needing clinical gait motion analysis.

Conflict of interest statement

We wish to confirm that there are no known conflicts of interest associated with this publication and there has been no significant financial support for this work that could have influenced its outcome.

Acknowledgement

This research was supported by Basic Science Research Program through the National Research Foundation of Korea (NRF) funded by the Ministry of Education, Science and Technology (NRF-2013R1A1A2009495).

References

- Barton, J., Lees, A., 1997. An application of neural networks for distinguishing gait patterns on the basis of hip-knee joint angle diagrams. *Gait and Posture* 5, 28–33.
- Barton, J., Lees, A., 1995. Development of a connectionist expert system to identify foot problems based on under-foot pressure patterns. *Clinical Biomechanics* 10, 385–391.
- Bowden, G.J., Dandy, G.C., Maier, H.R., 2005. Input determination for neural network models in water resources applications. Part 1—background and methodology. *Journal of Hydrology* 301, 75–92.
- Buczek, F.L., Rainbow, M.J., Cooney, K.M., Walker, M.R., Sanders, J.O., 2010. Implications of using hierarchical and six degree-of-freedom models for normal gait analyses. *Gait and Posture* 31, 57–63.
- Chau, T., Young, S., Redekop, S., 2005. Managing variability in the summary and comparison of gait data. *Journal of Neuroengineering and Rehabilitation* 2, 22.
- Davis, B.L., Cavanagh, P.R., 1993. Decomposition of superimposed ground reaction forces into left and right force profiles. *Journal of Biomechanics* 26, 593–597.
- Delen, D., Walker, G., Kadam, A., 2005. Predicting breast cancer survivability: a comparison of three data mining methods. *Artificial Intelligence in Medicine* 34, 113–127.
- Favre, J., Hayoz, M., Erhart-Hledik, J.C., Andriacchi, T.P., 2012. A neural network model to predict knee adduction moment during walking based on ground reaction force and anthropometric measurements. *Journal of Biomechanics* 45, 692–698.
- Fernando, T.M.K.G., Maier, H.R., Dandy, G.C., 2009. Selection of input variables for data driven models: an average shifted histogram partial mutual information estimator approach. *Journal of Hydrology* 367, 165–176.
- Gaggero, M., Gneco, G., Sanguineti, M., 2013. Dynamic programming and value-function approximation in sequential decision problems: error analysis and numerical results. *Journal of Optimization Theory and Applications* 156, 380–416.
- Goldberg, S.R., Ounpuu, S., Arnold, A.S., Gage, J.R., Delp, S.L., 2006. Kinematic and kinetic factors that correlate with improved knee flexion following treatment for stiff-knee gait. *Journal of Biomechanics* 39, 689–698.
- Holzreiter, S.H., Köhle, M.E., 1993. Assessment of gait patterns using neural networks. *Journal of Biomechanics* 26, 645–651.
- Islam, S., Kothari, R., 2000. Artificial neural networks in remote sensing of hydrologic processes. *Journal of Hydrologic Engineering* 5, 138–144.
- Kaczmarczyk, K., Wit, A., Krawczyk, M., Zaborski, J., 2009. Gait classification in post-stroke patients using artificial neural networks. *Gait and Posture* 30, 207–210.
- Kadaba, M.P., Ramakrishnan, H.K., Wootten, M.E., Gainey, J., Gorton, J., Cochran, G.V.B., 1989. Repeatability of kinematic, kinetic, and electromyographic data in normal adult gait. *Journal of Orthopaedic Research* 7, 849–860.
- Kadaba, M.P., Ramakrishnan, H.K., Wootten, M.E., 1990. Measurement of lower extremity kinematics during level walking. *Journal of Orthopaedic Research* 8, 383–392.
- Karimi, Y., Prasher, S.O., Patel, R.M., Kim, S.H., 2006. Application of support vector machine technology for weed and nitrogen stress detection in corn. *Computers and Electronics in Agriculture* 51, 99–109.
- Kohonen, T., 1982. Self-organized formation of topologically correct feature maps. *Biological Cybernetics* 43, 59–69.
- Kolmogorov, A.N., 1957. On the representation of continuous functions of many variables by superposition of continuous functions of one variable and addition. *Doklady Akademii Nauk SSSR* 114, 953–956. (Translations American Mathematical Society 28, 1963, 55–59).
- Lafuente, R., Belda, J., Sanchez-Lacuesta, J., Soler, C., Prat, J., 1998. Design and test of neural networks and statistical classifiers in computer-aided movement analysis: a case study on gait analysis. *Clinical Biomechanics* 13, 216–229.
- Liu, M.M., Herzog, W., Savelberg, H., 1999. Dynamic muscle force predictions from EMG: an artificial neural network approach. *Journal of Electromyography and Kinesiology* 9, 391–400.
- Liu, Y., Shih, S.M., Tian, S.L., Zhong, Y.J., Li, L., 2009. Lower extremity joint torque predicted by using artificial neural network during vertical jump. *Journal of Biomechanics* 42, 906–911.
- Lugris, U., Carlin, J., Pàmies-Vilà, R., Cuadrado, J., 2011. Comparison of methods to determinate ground reactions during the double support phase of gait. In: *Proceedings of the International Symposium on Multibody Systems and Mechatronics*, Spain.
- Mills, P.M., Morrison, S., Lloyd, D.G., Barrett, R.S., 2007. Repeatability of 3D gait kinematics obtained from an electromagnetic tracking system during treadmill locomotion. *Journal of Biomechanics* 40, 1504–1511.
- Nester, C., Van Der Linden, M., Bowker, P., 2003. Effect of foot orthoses on the kinematics and kinetics of normal walking gait. *Gait and Posture* 17, 180–187.
- Noori, R., Karbassi, A., Moghaddamnia, A., Han, D., Zokaei-Ashtiani, M., Farokhnia, A., Gousheh, M.G., 2011. Assessment of input variables determination on the SVM model performance using PCA, Gamma test, and forward selection techniques for monthly stream flow prediction. *Journal of Hydrology* 401, 177–189.
- O'Connor, C.M., Thorpe, S.K., O'Malley, M.J., Vaughan, C.L., 2007. Automatic detection of gait events using kinematic data. *Gait and Posture* 25, 469–474.
- Rao, G., Amarantini, D., Berton, E., Favier, D., 2006. Influence of body segments' parameters estimation models on inverse dynamics solutions during gait. *Journal of Biomechanics* 39, 1531–1536.
- Ren, L., Jones, R.K., Howard, D., 2008. Whole body inverse dynamics over a complete gait cycle based only on measured kinematics. *Journal of Biomechanics* 41, 2750.
- Ren, L., Jones, R.K., Howard, D., 2005. Dynamic analysis of load carriage biomechanics during level walking. *Journal of Biomechanics* 38, 853–863.
- Riemer, R., Hsiao-Weckler, E.T., Zhang, X., 2008. Uncertainties in inverse dynamics solutions: a comprehensive analysis and an application to gait. *Gait and Posture* 27, 578–588.
- Schalkoff, R.J., 1997. *Artificial Neural Networks*. McGraw-Hill, New York.
- Schöllhorn, W., 2004. Applications of artificial neural nets in clinical biomechanics. *Clinical Biomechanics* (Bristol, Avon) 19, 876.
- Senden, R., Grimm, B., Heyligers, I., Savelberg, H., Meijer, K., 2009. Acceleration-based gait test for healthy subjects: reliability and reference data. *Gait and Posture* 30, 192–196.
- Siegler, S., Liu, W., 1997. Inverse dynamics in human locomotion. In: Allard, P., et al. (Eds.), *Three Dimensional Analysis of Human Locomotion*. Wiley, New York, pp. 191–209.
- Sofuwa, O., Nieuwboer, A., Desloovere, K., Willems, A.M., Chavret, F., Jonkers, I., 2005. Quantitative gait analysis in Parkinson's disease: comparison with a healthy control group. *Archives of Physical Medicine and Rehabilitation* 86, 1007–1013.
- Vijayakumar, G., Ramamurthy, V., 2013. Artificial neural network model for predicting production of *Spirulina platensis* in outdoor culture. *Bioresource Technology* 130, 224–230.
- Winter, D.A., 1991. *Biomechanics and Motor Control of Human Gait: Normal, Elderly and Pathological*, 2nd Ed. University of Waterloo Press.
- Winter, D.A., 2009. *Biomechanics and Motor Control of Human Movement*. Wiley, New York.
- Xiang, Y., Arora, J.S., Abdel-Malek, K., 2011. Optimization-based prediction of asymmetric human gait. *Journal of Biomechanics* 44, 683–693.